

Dear Author

Here are the proofs of your article.

- You can submit your corrections **online**, via **e-mail** or by **fax**.
- For **online** submission please insert your corrections in the online correction form. Always indicate the line number to which the correction refers.
- You can also insert your corrections in the proof PDF and **email** the annotated PDF.
- For **fax** submission, please ensure that your corrections are clearly legible. Use a fine black pen and write the correction in the margin, not too close to the edge of the page.
- Remember to note the **journal title**, **article number**, and **your name** when sending your response via e-mail or fax.
- **Check** the metadata sheet to make sure that the header information, especially author names and the corresponding affiliations are correctly shown.
- **Check** the questions that may have arisen during copy editing and insert your answers/corrections.
- **Check** that the text is complete and that all figures, tables and their legends are included. Also check the accuracy of special characters, equations, and electronic supplementary material if applicable. If necessary refer to the *Edited manuscript*.
- The publication of inaccurate data such as dosages and units can have serious consequences. Please take particular care that all such details are correct.
- Please **do not** make changes that involve only matters of style. We have generally introduced forms that follow the journal's style.
- Substantial changes in content, e.g., new results, corrected values, title and authorship are not allowed without the approval of the responsible editor. In such a case, please contact the Editorial Office and return his/her consent together with the proof.
- If we do not receive your corrections **within 48 hours**, we will send you a reminder.
- Your article will be published **Online First** approximately one week after receipt of your corrected proofs. This is the **official first publication** citable with the DOI. **Further changes are, therefore, not possible.**
- The **printed version** will follow in a forthcoming issue.

Please note

After online publication, subscribers (personal/institutional) to this journal will have access to the complete article via the DOI using the URL:

If you would like to know when your article has been published online, take advantage of our free alert service. For registration and further information, go to:
<http://www.link.springer.com>.

Due to the electronic nature of the procedure, the manuscript and the original figures will only be returned to you on special request. When you return your corrections, please inform us, if you would like to have these documents returned.

Metadata of the article that will be visualized in OnlineFirst

1	Article Title	Freeze/thaw stress induces organelle remodeling and membrane recycling in cryopreserved human mature oocytes	
2	Article Sub- Title		
3	Article Copyright - Year	Springer Science+Business Media New York 2016 (This will be the copyright line in the final PDF)	
4	Journal Name	Journal of Assisted Reproduction and Genetics	
5	Corresponding Author	Family Name	Nottola
6		Particle	
7		Given Name	Stefania Annarita
8		Suffix	
9		Organization	Sapienza University
10		Division	Department of Anatomy, Histology, Forensic Medicine and Orthopaedics
11		Address	Rome
12		e-mail	stefania.nottola@uniroma1.it
13	Author	Family Name	Albani
14		Particle	
15		Given Name	Elena
16		Suffix	
17		Organization	Humanitas Research Hospital, Department of Gynecology, Division of Gynecology and Reproductive Medicine, Humanitas Fertility Center
18		Division	
19		Address	Rozzano, Milan
20		e-mail	
21	Author	Family Name	Coticchio
22		Particle	
23		Given Name	Giovanni
24		Suffix	
25		Organization	Tecnobios Procreazione, Centre for Reproductive Health
26		Division	
27		Address	Bologna

28		Organization	Biogenesi, Reproductive Medicine Centre
29		Division	
30		Address	Monza
31		e-mail	
<hr/>			
32		Family Name	Palmerini
33		Particle	
34		Given Name	Maria Grazia
35		Suffix	
36		Organization	University of L'Aquila
37	Author	Division	Department of Life, Health and Environmental Sciences
38		Address	L'Aquila
39		Organization	Biogenesi, Reproductive Medicine Centre
40		Division	
41		Address	Monza
42		e-mail	
<hr/>			
43		Family Name	Lorenzo
44		Particle	
45		Given Name	Caterina
46		Suffix	
47	Author	Organization	University of L'Aquila
48		Division	Department of Life, Health and Environmental Sciences
49		Address	L'Aquila
50		e-mail	
<hr/>			
51		Family Name	Scaravelli
52		Particle	
53		Given Name	Giulia
54		Suffix	
55	Author	Organization	CNESPS, National Health Institute
56		Division	
57		Address	Rome
58		e-mail	
<hr/>			
59		Family Name	Borini
60	Author	Particle	
61		Given Name	Andrea
62		Suffix	

63		Organization	Tecnobios Procreazione, Centre for Reproductive Health
64		Division	
65		Address	Bologna
66		e-mail	
<hr/>			
67		Family Name	Levi-Setti
68		Particle	
69		Given Name	Paolo Emanuele
70		Suffix	
71	Author	Organization	University of L'Aquila
72		Division	Department of Life, Health and Environmental Sciences
73		Address	L'Aquila
74		e-mail	
<hr/>			
75		Family Name	Macchiarelli
76		Particle	
77		Given Name	Guido
78		Suffix	
79	Author	Organization	University of L'Aquila
80		Division	Department of Life, Health and Environmental Sciences
81		Address	L'Aquila
82		e-mail	
<hr/>			
83		Received	21 July 2016
84	Schedule	Revised	
85		Accepted	16 August 2016
<hr/>			
86	Abstract	<p>Purpose: Cryopreservation may affect oocyte morphology and competence. Little is known about influence of thawing and rehydration on oocyte integrity. Our aim was to evaluate the ultrastructure of human metaphase II oocytes subjected to slow freezing and fixed after thawing at different intervals during post-thaw rehydration.</p> <p>Methods: Samples were studied by light and transmission electron microscopy.</p> <p>Results: We found that vacuolization was present in all cryopreserved oocytes, reaching a maximum in the intermediate stage of rehydration. Mitochondria-smooth endoplasmic reticulum (M-SER) aggregates decreased following thawing, particularly in the first and intermediate stages of rehydration, whereas mitochondria-vesicle (MV) complexes augmented in the same stages. At the end of rehydration, vacuoles and MV complexes both diminished and M-SER aggregates increased again. Cortical</p>	

granules (CGs) were scarce in all cryopreserved oocytes, gradually diminishing as rehydration progressed.

Conclusions: In conclusion, (a) vacuoles may form during freezing and/or at thawing but increase during rehydration; (b) significant changes of opposite trend in the number of M-SER aggregates and MV complexes occur during freeze-thawing; (c) CG exocytosis proceeds during the whole freeze-thawing procedure. Thus, all ooplasmic membranes appear influenced by freeze-thawing. However, except for CGs, membrane alterations seem to undergo a partial or, more rarely, an almost complete recovery at the end of the rehydration. This study also shows that such a membrane remodeling is mainly represented by a dynamic process of transition between M-SER aggregates and MV complexes, both able of transforming into each other. Vacuoles and CG membranes may take part in the membrane recycling mechanism.

87 **Keywords** Oocyte - Vacuoles - Organelles - Cryopreservation - Human -
 separated by ' - ' Ultrastructure

88 **Foot note**
 information

1
3
2

4
5

Freeze/thaw stress induces organelle remodeling and membrane recycling in cryopreserved human mature oocytes

6
7
8
9

Stefania Annarita Nottola¹ · Elena Albani² · Giovanni Coticchio^{3,4} ·
Maria Grazia Palmerini⁵ · Caterina Lorenzo⁵ · Giulia Scaravelli⁶ · Andrea Borini³ ·
Paolo Emanuele Levi-Setti⁵ · Guido Macchiarelli⁵

10
11

Received: 21 July 2016 / Accepted: 16 August 2016
© Springer Science+Business Media New York 2016

12
13
14
15
16
17
18
19
20
21
22
23
24
25
26
27
28
29

Abstract

Purpose Cryopreservation may affect oocyte morphology and competence. Little is known about influence of thawing and rehydration on oocyte integrity. Our aim was to evaluate the ultrastructure of human metaphase II oocytes subjected to slow freezing and fixed after thawing at different intervals during post-thaw rehydration.

Methods Samples were studied by light and transmission electron microscopy.

Results We found that vacuolization was present in all cryopreserved oocytes, reaching a maximum in the intermediate stage of rehydration. Mitochondria-smooth endoplasmic reticulum (M-SER) aggregates decreased following thawing, particularly in the first and intermediate stages of rehydration, whereas mitochondria-vesicle (MV) complexes augmented in the same stages. At the end of rehydration, vacuoles and MV complexes both diminished and M-SER aggregates increased again. Cortical granules (CGs) were scarce in all

cryopreserved oocytes, gradually diminishing as rehydration progressed. *Conclusions* In conclusion, (a) vacuoles may form during freezing and/or at thawing but increase during rehydration; (b) significant changes of opposite trend in the number of M-SER aggregates and MV complexes occur during freeze-thawing; (c) CG exocytosis proceeds during the whole freeze-thawing procedure. Thus, all ooplasmic membranes appear influenced by freeze-thawing. However, except for CGs, membrane alterations seem to undergo a partial or, more rarely, an almost complete recovery at the end of the rehydration. This study also shows that such a membrane remodeling is mainly represented by a dynamic process of transition between M-SER aggregates and MV complexes, both able of transforming into each other. Vacuoles and CG membranes may take part in the membrane recycling mechanism.

Keywords Oocyte · Vacuoles · Organelles · Cryopreservation · Human · Ultrastructure 46
47 **Q2**

✉ Stefania Annarita Nottola
stefania.nottola@uniroma1.it

Introduction 48

Oocyte cryopreservation currently represents a valuable procedure among assisted reproductive technologies (ART) that bypasses some ethical, moral, and religious dilemmas associated with the storage of embryos. It is a valid solution for women who have to repeat in vitro fertilization (IVF) treatments avoiding the risk of ovarian hyperstimulation syndrome, and for women who may lose their ovarian function due to surgery, cancer treatments, or premature menopause [1]. Oocyte cryostorage may also represent a possibility to counteract future infertility for healthy women who decided to postpone childbearing due to educational or socio-economic pressures (social freezing) [2]. Despite such a

Q1

¹ Department of Anatomy, Histology, Forensic Medicine and Orthopaedics, Sapienza University, Rome, Italy
² Humanitas Research Hospital, Department of Gynecology, Division of Gynecology and Reproductive Medicine, Humanitas Fertility Center, Rozzano, Milan, Italy
³ Tecnobios Procreazione, Centre for Reproductive Health, Bologna, Italy
⁴ Present address: Biogenesi, Reproductive Medicine Centre, Monza, Italy
⁵ Department of Life, Health and Environmental Sciences, University of L'Aquila, L'Aquila, Italy
⁶ CNESPS, National Health Institute, Rome, Italy

61 paramount impact of oocyte cryopreservation, the mature, 114
62 metaphase II (MII) human oocyte is difficult to cryopreserve 115
63 [3]. This is due to oocyte peculiar features, such as large size 116
64 (low surface-to-volume ratio), high water content, elevated 117
65 degree of cytoplasmic specialization, and sensitivity of the 118
66 chromosome segregation machinery [4–9]. Indeed, some 119
67 structural domains of the mammalian MII oocytes, such as 120
68 zona pellucida (ZP), cortical granules (CGs), and other organ- 121
69 elles, cytoskeletal components and, particularly, meiotic spin- 122
70 dle are sensitive to the process of cryopreservation, due to the 123
71 negative effects exerted by low temperatures, formation of 124
72 intracellular ice crystals, osmotic stress, and toxicity of the 125
73 substances used as cryoprotectants (for references, see: 126
74 [10–17]). Thus, light and transmission electron microscopy 127
75 (LM and TEM) are powerful tools of investigation and eval- 128
76 uation of the impact that the above factors may have on human 129
77 oocyte microstructure during freeze-thawing. 130

78 Vacuolization from a slight to a moderate extent is an 131
79 important dysmorphism that has been frequently detected 132
80 by both LM and TEM in the ooplasm of human mature 133
81 oocytes subjected to cryopreservation, mainly when slow 134
82 freezing is applied [12, 17, 18]. Vacuoles are also present 135
83 in aging or degenerating oocytes, whereas in fresh, healthy 136
84 MII oocytes they are very scarce or virtually absent 137
85 [19–23]. Thus, the occurrence of vacuolization in frozen- 138
86 thawed oocytes may be considered a form of structural 139
87 damage explainable as a non-specific response of the oo- 140
88 cyte to cryoinjury and/or osmotic stress. In addition, since 141
89 oocytes subjected to different protocols of slow freezing 142
90 may show different degrees of vacuolization [12–14, 17, 143
91 24, 25], it should not be ruled out that oocyte vacuolization 144
92 may be dependent, at least in part, upon the type and/or 145
93 concentration of the cryoprotectants. Oocyte 146
94 dysmorphisms may be related to poor clinical outcomes 147
95 [26]. Although the effects of oocyte vacuolar dysmorphism 148
96 on embryo development may remain controversial [27], it 149
97 is a common finding that vacuolated MII oocytes show 150
98 poor fertilization rates [28]. If fertilized, vacuolated oo- 151
99 cytes may show reduced cleavage or arrested development 152
100 [22, 29, 30]. However, while oocyte vacuolization seems 153
101 to be associated with IVF failure, the genesis of vacuoles 154
102 and the morphodynamics of vacuole formation have not 155
103 yet been fully understood.

104 Well-defined composite associations between mito- 156
105 chondria and cytoplasmic membranes are characteristically 157
106 found in the ooplasm of fully grown human oocytes, 158
107 named mitochondria-smooth endoplasmic reticulum (M- 159
108 SER) aggregates and mitochondria-vesicle (MV) com- 160
109 plexes [19, 22, 31, 32]. Mitochondria and associated cyto- 161
110 plasmic membranes may play a role in production of sub- 162
111 stances useful at fertilization and/or in rapid neof ormation 163
112 of membranes during early embryogenesis [20, 33, 34]. M- 164
113 SER aggregates may also regulate local levels of free 165

114 calcium and ATP production, thus acting on different cel- 115
116 lular activities including the mediation of an “explosive” 117
118 calcium signal at fertilization [23, 35–38]. Thus, distur- 119
120 bances in morphology and function of these organelle as- 121
122 sociations may lead to a reduced oocyte competence for 123
124 fertilization. In this regard, the presence of very large M- 125
126 SER aggregates, sometimes related to gonadotropin hyper- 127
128 stimulation [21], has been generally associated with com- 129
130 promised embryo development and implantation [39, 40], 131
132 even though different opinions have been recently 133
134 expressed [41–43]. On the contrary, underdeveloped M- 135
136 SER aggregates have been found in a percentage of human 137
138 mature oocytes subjected to vitrification [15] or to a slow 139
140 freezing protocol based on the use of ethylene glycol as 141
142 cryoprotectant agent [14], whereas other studies on slow- 143
144 frozen oocytes treated with propanediol (PrOH) did not 144
145 evidence qualitatively detectable ultrastructural alterations 145
146 in M-SER aggregates [12, 13, 17]. However, a quantitative 146
147 morphometric analysis on mitochondria and associated 147
148 membranes has not been carried out up to now in human 148
149 cryopreserved oocytes. 149

150 Several researchers, using TEM, have identified an 151
152 abnormal reduction of the amount of CGs in mature oo- 153
154 cytes of some mammals, including humans, after the ap- 154
155 plication of different cryopreservation protocols [12–15, 155
156 17, 24, 44–49]. Ultrastructural evidence of premature CG 157
158 release has been also found after the simple contact of 158
159 the oocyte with some cryoprotectants, as described by 159
160 Schalkoff et al. [50] in human oocytes exposed to either 160
161 1,2-PrOH or dimethylsulfoxide at room temperature 161
162 (RT). Contrasting data have been reported by Jones 162
163 et al. [51], who found an abundance of CGs in the 163
164 ooplasm of human PrOH-cryopreserved oocytes, al- 164
165 though these observations do not preclude the possibility 165
166 that a partial CG exocytosis in some other areas would 166
167 not be detected. Thus, keeping under observation the 167
168 presence and amount of CGs in human oocytes after 168
169 the freeze-thawing procedure is extremely important. In 169
170 fact, precocious oocyte activation—with a consequent 170
171 decrement of oocyte developmental competence—is a 171
172 phenomenon that may eventually be demonstrated with 172
173 the appearance of premature CG exocytosis [15]. 173

174 With the aim to give a contribution in solving some ques- 175
176 tions related to the quality, timing, and entity of organelle 176
177 alterations occurring during human oocyte cryopreservation, 177
178 the present report was intended to evaluate presence and 178
179 amount of (a) ooplasmic vacuolization, (b) organelle-specific 179
180 associations such as M-SER aggregates and MV complexes, 180
181 and (c) CGs in human MII oocytes subjected to slow freezing 181
182 and examined after thawing, at different intervals during post- 182
183 thaw rehydration. Morphological data have been collected and 183
184 evaluated though an integrated LM, TEM and morphometric 184
185 approach. 185
186

167	Materials and methods	
168	Source of oocytes	
169	This study was approved by Institutional Review Board of	
170	the participating Clinics. Surplus oocytes, donated for re-	
171	search purpose, were obtained over a period between	
172	July 2008 and September 2010 from patients undergoing	
173	ART treatment, with high number of oocytes and after their	
174	informed consent, according to the current Italian laws.	
175	Only oocytes provided by women ($N=32$) younger than	
176	33 years (mean \pm standard deviation, SD: 31.36 ± 1), whose	
177	infertility was due to male or disovulatory factors, were	
178	used. Controlled ovarian hyperstimulation was induced	
179	with long protocols using GnRH agonist and rFSH, accord-	
180	ing to the standard clinical procedures routinely employed	
181	by the participating Clinics [52]. Ten thousand IU of hCG	
182	were administered 36 h prior to oocyte collection. After	
183	retrieval, oocytes were cultured in IVF media (Cook IVF,	
184	Brisbane, Australia, or Sage IVF Inc, Trumbull, CT, USA).	
185	Complete removal of cumulus mass and corona cells was	
186	performed enzymatically using hyaluronidase (80 IU/ml),	
187	and mechanically by using fine bore glass pipettes. Only	
188	oocytes devoid of any dysmorphism at phase contrast mi-	
189	croscopy (PCM) examination, showing an extruded first	
190	polar body (PBI), thus presumably at the MII stage, were	
191	assigned to the control or experimental groups. According	
192	to their assignment, oocytes were either frozen or fixed	
193	after a period of 3–4 h following retrieval.	
194	Freezing procedure	
195	Freezing was performed according to the two-step PrOH	
196	dehydration. In detail, the oocytes were equilibrated se-	
197	quentially in solutions containing respectively 0.75 mol/l	
198	PrOH + 20 % plasma protein supplement (PPS) and	
199	1.5 mol/l PrOH + 20 % PPS in Dulbecco's phosphate-	
200	buffered saline (PBS) (7.5 min for each step). Further, oo-	
201	cytes were transferred for 5 min into the loading solution	
202	(1.5 mol/l PrOH + 0.2 mol/l sucrose + 20 % PPS in PBS).	
203	Oocytes were finally loaded in plastic straws (Paillettes	
204	Crystal 133 mm; Cryo Bio System, France), individually	
205	or in small groups (maximum three oocytes per straw).	
206	Straw temperature was lowered through an automated	
207	Kryo 10 series III biological freezer (Planer Kryo 10/	
208	1,7 GB) from 20 to -8 °C at a rate of -2 °C/min).	
209	Manual seeding was performed at -8 °C. This temperature	
210	was maintained in a hold interval of 10 min in order to	
211	allow uniform ice propagation. Temperature was then de-	
212	creased to -30 °C at a rate of -0.3 °C/min and finally	
213	rapidly to -150 °C at a rate of -50 °C/min. Finally, straws	
214	were directly plunged into liquid nitrogen and stored for	
215	later use.	
	Thawing procedure	216
	Thawing was carried out at RT. Straws were removed from	217
	liquid nitrogen, warmed in air for 30 s and then plunged in a	218
	water bath at 37 °C for 40 s. The thawing solutions contained a	219
	gradually decreasing concentration of PrOH and a constant	220
	0.3 mol/l sucrose concentration. Thawed oocytes were firstly	221
	released in 1.0 mol/l PrOH + 0.3 mol/l sucrose + 20 % PPS	222
	(solution 1) and incubated for 5 min. Afterwards, they were	223
	transferred in 0.5 mol/l PrOH + 0.3 mol/l sucrose + 20 % PPS	224
	(solution 2) for additional 5 min. Finally, oocytes were placed	225
	in 0.3 mol/l sucrose + 20 % PPS (solution 3) for 10 min before	226
	final dilution in PBS + 20 % PPS (solution 4) for 20 min	227
	(10 min at RT and 10 min at 37 °C). All freezing and thawing	228
	solutions were manufactured by Cook IVF, Brisbane,	229
	Australia.	230
	Electron microscopy	231
	Only oocytes with highest morphological scores at PCM ex-	232
	amination [53] were selected for electron microscopy analy-	233
	sis. A total of 60 MII oocytes were included in this study.	234
	Fifteen of them were fixed after 3–4 h following retrieval	235
	and assigned to the control group. The other 45 oocytes, after	236
	being cultured for 4 h, were subjected to freeze-thawing as	237
	described above and fixed in glutaraldehyde after thawing,	238
	at different intervals during post-thaw rehydration, as follows:	239
	group A, oocytes fixed after the passage in thawing solution 1	240
	($N=15$); group B, oocytes fixed after the passage in thawing	241
	solution 2 ($N=15$); group C, oocytes fixed after the passage in	242
	thawing solution 3 ($N=15$).	243
	Oocytes were processed for LM and TEM as previously	244
	described [12–15, 54]. Oocyte fixation was performed in	245
	1.5 % glutaraldehyde (SIC, Rome, Italy) in PBS solution.	246
	After fixation for 2–5 days at 4 °C, the samples were rinsed	247
	in PBS, post-fixed with 1 % osmium tetroxide (Agar	248
	Scientific, Stansted, UK) in PBS, and rinsed again in PBS.	249
	Oocytes were then embedded in small blocks of 1 % agar of	250
	about $5 \times 5 \times 1$ mm in size, dehydrated in ascending series of	251
	ethanol (Carlo Erba Reagenti, Milan, Italy), immersed in pro-	252
	pylene oxide (BDH Italia, Milan, Italy) for solvent substitu-	253
	tion, embedded in Epoxy resin (Agar Scientific, Stansted, UK)	254
	and sectioned by a Reichert-Jung Ultracut E ultramicrotome.	255
	Semithin sections (1- μ m thick) were stained with toluidine	256
	blue, examined by LM (Zeiss Axioskop) and photographed	257
	using a digital camera (Leica DFC230). Ultrathin sections	258
	(60–80 nm) were cut with a diamond knife, mounted on cop-	259
	per grids, and contrasted with saturated uranyl acetate follow-	260
	ed by lead citrate (SIC, Rome, Italy). The ultrathin sections	261
	were examined and photographed using a Zeiss EM 10 and a	262
	Philips TEM CM100 Electron Microscopes operating at	263
	80KV. Images were acquired using a GATAN charge-	264
	coupled device camera.	265

266 **Ultrastructural parameters**

267 The following parameters were evaluated by LM and TEM
 268 and taken into consideration for the qualitative morphological
 269 assessment of the structural and ultrastructural preservation of
 270 oocytes: general features (including shape and dimensions),
 271 presence and extent of ooplasmic vacuolization,
 272 microtopography, type and quality of the organelles, integrity
 273 of the oolemma, ZP texture, and appearance of the
 274 perivitelline space (PVS) [15, 55].

275 PBI and MII spindle features were not systematically
 276 assessed by LM and TEM due to their detection only in sections
 277 lying on appropriate planes.

278 **Statistical analysis**

279 The presence of vacuoles, M-SER aggregates, and MV com-
 280 plexes was evaluated at the LM level on at least 3 equatorial
 281 semithin sections per oocyte (distance between the sections:
 282 3–4 μm). For each section, counting was performed on a
 283 single panoramic image of each oocyte, obtained combining
 284 together several pictures of different oocyte portions taken
 285 at $\times 100$ magnification by using the function Photoshop's
 286 Photomerge (PS Adobe Photoshop CS3). The amount of vacu-
 287 oles, M-SER aggregates and MV complexes was expressed
 288 in number of vacuoles or organelle associations per $100 \mu\text{m}^2$
 289 of the oocyte area. Only structures (vacuoles, SER networks,
 290 vesicles) greater than or equal to $0.5 \mu\text{m}$ in diameter were
 291 counted.

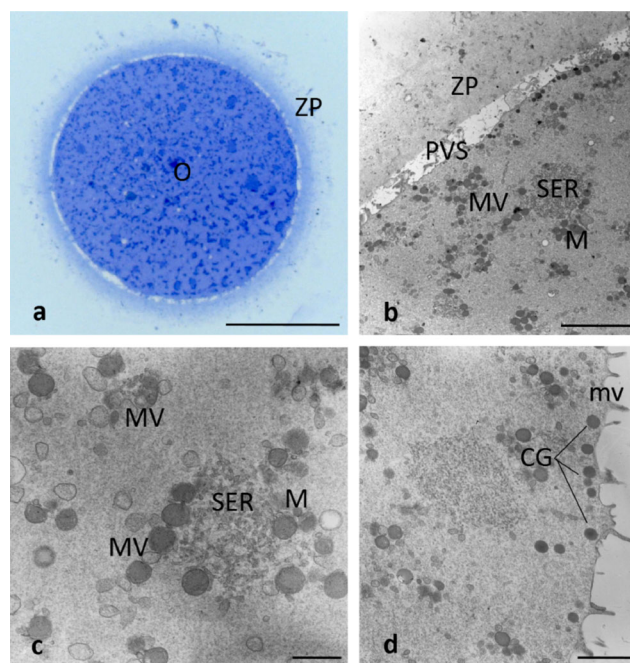
292 The evaluation of CG density was performed through col-
 293 lection of TEM micrographs of whole surface profiles
 294 at $\times 6300$ magnification on 3 equatorial ultrathin sections per
 295 oocyte. The images were further magnified on the PC screen
 296 to easily recognize and count CGs. Values were expressed as
 297 the number of CGs for $10 \mu\text{m}$ of the oocyte linear surface
 298 profile [12, 15, 25].

299 All data were expressed as mean \pm SD and compared by
 300 one-way analysis of variance (ANOVA) and Tukey's test as
 301 post hoc test (GraphPad InStat). Differences in values were
 302 considered significant if $P < 0.05$.

303 **Results**

304 **Control oocytes**

305 A total of 15 fresh, control oocytes were observed. When
 306 analyzed by LM, these oocytes appeared rounded in shape,
 307 90–100 μm in diameter (ZP excluded), provided with a
 308 homogeneously textured ooplasm in which vacuoles were
 309 rarely seen (Fig. 1a). Morphometric analysis revealed that
 310 the mean number \pm SD of vacuoles per $100 \mu\text{m}^2$ was 1.06
 311 ± 0.18 in the control group (Fig. 3d). By LM and low



312 **Fig. 1** Fresh human metaphase II oocytes. The general features and
 313 organelle microtopography are shown by light (Fig. 1a) and
 314 transmission (TEM) (Fig. 1b) electron microscopy. Note the rounded
 315 shape of the oocyte (O), the narrow perivitelline space (PVS), the intact
 316 zona pellucida (ZP) and the uniform distribution of organelles in the
 317 ooplasm. Among the organelles, numerous mitochondria (M),
 318 mitochondria-smooth endoplasmic reticulum (M-SER) aggregates and
 319 mitochondria-vesicle (MV) complexes can be found. By TEM, details
 320 of a M-SER aggregate and of several, small MV complexes are seen in
 321 Fig. 1c. A rim of cortical granules (CG) is also seen just beneath the
 322 oolemma in Fig. 1d. mv microvilli. Bar is: 45 μm (Fig. 1a); 5 μm
 323 (Fig. 1b); 1 μm (Fig. 1c); 2 μm (Fig. 1d)

324 magnification TEM the organelles, including numerous,
 325 large M-SER aggregates and small MV complexes, ap-
 326 peared scattered in the ooplasm (Fig. 1a, b). By morpho-
 327 metric analysis, the mean number \pm SD of M-SER found in
 328 $100 \mu\text{m}^2$ was 0.96 ± 0.01 while the mean number \pm SD of
 329 MV in $100 \mu\text{m}^2$ was 0.60 ± 0.29 (Figs. 4b; 5c). A contin-
 330 uous, intact ZP, approximately 10–12- μm thick, complet-
 331 ely surrounded the oocyte, which was separated from the
 332 inner zona aspect by a narrow PVS (Fig. 1a, b). By TEM,
 333 mitochondria (0.5–1 μm in diameter), rounded or oval—in
 relation to the orientation of the cutting section—and pro-
 vided with arched *cristae*, were numerous and characteris-
 tically associated with networked SER tubules with a di-
 ameter varying from 1 to 5 μm , forming the M-SER ag-
 gregates (Fig. 1b, c). MV complexes appeared as small
 vesicles with a diameter of about 0.5 μm , filled with flo-
 culent, slightly electrondense material and surrounded by
 mitochondria (Fig. 1b, c). Rounded, electrondense CGs,
 varying in diameter from 300 to 400 nm, were abundant
 and stratified in one/two layers in suboolemmal areas
 (mean number \pm SD of CGs per $10 \mu\text{m}$ = 9.07 ± 0.45)
 (Figs. 1d; 6d).

334 Numerous microvilli of variable length projected from the
 335 oolemma into the PVS (Fig. 1d). In sections lying on appropriate
 336 planes, the PBI was detected in the PVS and the MII
 337 spindle was found in the ooplasm.

338 **Cryopreserved oocytes**

339 In total, 45 mature cryopreserved oocytes, 15 for each exper-
 340 imental group (A, B, C), were analyzed. A preliminary eval-
 341 uation was performed by LM (Fig. 2a–c). All the oocytes
 342 were rounded, with a diameter ranging from 90 to 100 μm ,
 343 provided with a homogeneous ooplasm and surrounded by a
 344 regular, uninterrupted ZP. No overt differences in oocyte
 345 shape/dimensions were detected between cryopreserved and control
 346 oocytes and among cryopreserved oocytes belonging
 347 to different experimental groups.

348 By LM, circular areas of different sizes and shapes in
 349 which staining and matter consistency were reduced, identi-
 350 fied as vacuoles, were numerous in the ooplasm of the cryo-
 351 preserved oocytes belonging to all the experimental groups
 352 (Fig. 2). With regard to their distribution, vacuoles populated
 353 both inner and outer oocyte areas, but appeared more concen-
 354 trated in the deeper ooplasm. Morphometric analysis revealed
 355 that the mean number \pm SD of vacuoles per 100 μm^2 was
 356 7.20 ± 1.50 (group A), 17.05 ± 5.50 (group B), 9.50 ± 5.20
 357 (group C). Thus, vacuoles were numerous in group A (differ-
 358 ence between control group and group A was statistically
 359 significant, $P < 0.001$). In addition, vacuoles further increased
 360 with the progression of rehydration, reaching a maximum
 361 amount in group B (difference between groups A and B
 362 was statistically significant, $P < 0.05$) and diminishing again
 363 at the end of the rehydration process (difference between
 364 groups A and C was not statistically significant, $P = 0.3$)
 365 (Fig. 3d).

366 By LM and low magnification TEM, the organelles ap-
 367 peared evenly dispersed in the ooplasm of all frozen-thawed
 368 oocytes, as in the control samples, irrespective of the exper-
 369 imental group (A, B, C) (Fig. 2). However, M-SER aggre-
 370 gates significantly diminished following thawing, and such a
 371 decrease in number was particularly evident in the oocytes
 372 belonging to groups A and B. In fact, the mean number \pm SD
 373 of M-SER was 0.20 ± 0.03 in group A (control vs group A,
 374 $P < 0.001$) and 0.04 ± 0.03 in group B (control vs group B,
 375 $P < 0.001$) (Fig. 4b). On the contrary, MV complexes, small
 376 and scarce in control oocytes, augmented in number after
 377 thawing, being especially abundant in the oocytes belonging
 378 to group B. Specifically, the mean number \pm SD of MV in
 379 100 μm^2 was 1.12 ± 0.40 in group A (control vs group A,
 380 $P < 0.05$) and 2.36 ± 0.42 in group B (control vs group B,
 381 $P < 0.001$) (Fig. 5c). At the end of the rehydration process,
 382 organelle associations showed an opposite trend: in fact, M-
 383 SER aggregates increased again in number—though never
 384 reaching the abundance shown in control oocytes—whereas

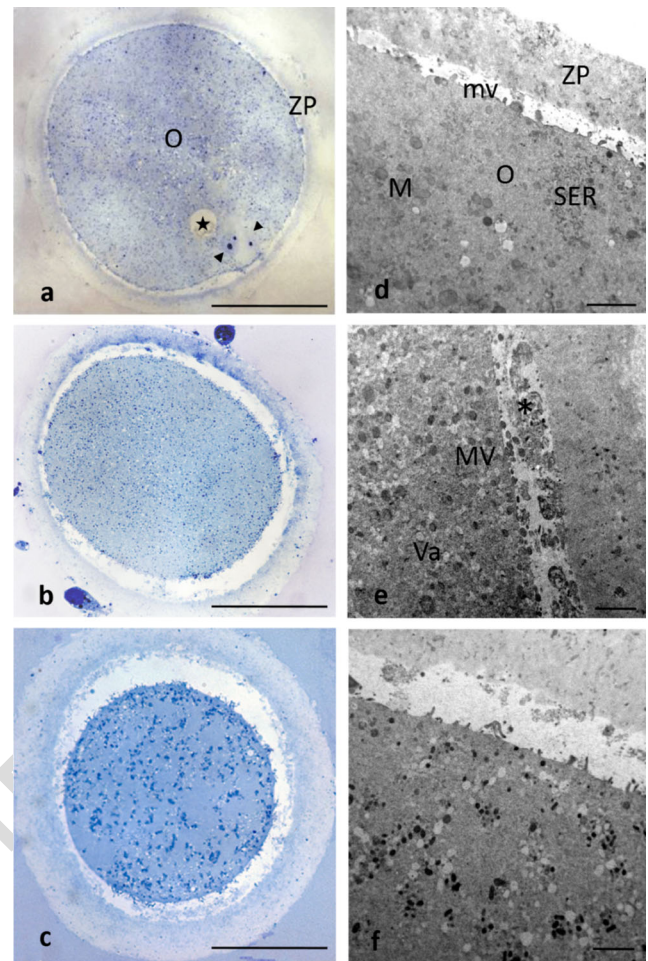


Fig. 2 Cryopreserved human metaphase II (MII) oocytes. By light (Fig. 2a–c) and transmission (Fig. 2d–f) electron microscopy, no overt difference in shape, dimensions, and organelle distribution is seen among the oocytes (O) belonging to group A (Fig. 2a, d), B (Fig. 2b, e), and C (Fig. 2c, f) and between fresh (see Fig. 1) and cryopreserved oocytes (Fig. 2). Note the intact zona pellucida (ZP) (Fig. 2a–c) and the presence of microvilli (mv) on the oolemma (Fig. 2d–f). Numerous vacuoles (Va) are seen in all cryopreserved oocytes, particularly abundant in group B (Fig. 2b, e). The apparent reduced dimensions, enlargement of the perivitelline space, and increased ZP thickness of the oocyte shown in Fig. 2c are effects of the section plane (not equatorial). arrowheads MII spindle with chromosomes, star large vacuole possibly due to a gas bubble, M mitochondria, SER smooth endoplasmic reticulum, MV mitochondria-vesicle complexes, asterisk remnants of the first polar body. Bar is: 45 μm (Fig. 2a); 40 μm (Fig. 2b); 35 μm (Fig. 2c); 2 μm (Fig. 2d–f)

MV complexes diminished in the oocytes belonging to group 385
 C, being respectively 0.87 ± 0.05 (control vs group C, 386
 $P < 0.001$) and 0.67 ± 0.29 (control vs group C, $P = 0.6$) 387
 (Figs. 4b; 5c). 388

By TEM, vacuoles, ranging in size from 0.5 to 4 μm , ap- 389
 peared delimited by membranes that were at times interrupted 390
 and characterized, in some parts, by densely organized inden- 391
 tations or niches. The inside of these compartments was 392
 scarcely electron-dense in comparison to the surrounding cy- 393
 toplasm and occasionally contained cell debris (Fig. 3a–c). 394

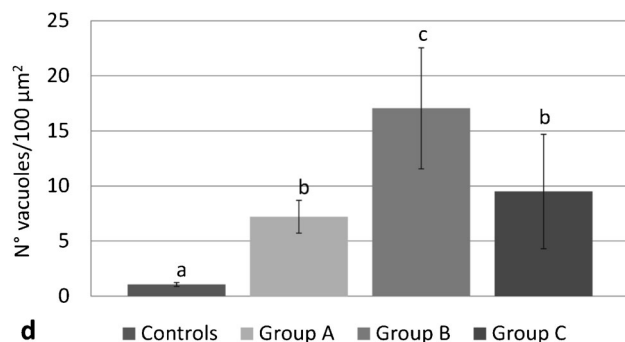
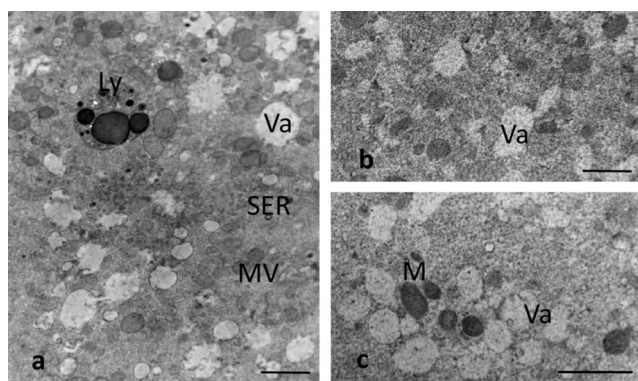


Fig. 3 Cryopreserved human metaphase II oocytes. By transmission electron microscopy, vacuoles (*Va*) are present in the ooplasm of the cryopreserved oocytes belonging to group A (Fig. 3a), B (Fig. 3b), and C (Fig. 3c). Vacuoles frequently appear empty (Fig. 3a–c) and may be delimited by a discontinuous membrane (Fig. 3a). A close association between vacuoles and lysosomes (*Ly*) is seen in Fig. 3a. Mitochondria (*M*), smooth endoplasmic reticulum (*SER*) networks and mitochondria-vesicle (*MV*) complexes are seen in the areas among vacuoles (Fig. 3a, c). Note the increased density of the cytoplasmic matrix in group b (Fig. 3b) in comparison with fresh controls (Fig. 1b–d) and groups a and c (Fig. 3a, c). Bar is: 1 μm (Fig. 3a–c). Fig. 3d: Number of vacuoles (vacuole diameter ≥ 0.5 μm) per 100 μm² of oocyte area. Values for each group are expressed as mean ± SD. Different letters indicate significant differences ($P < 0.05$)

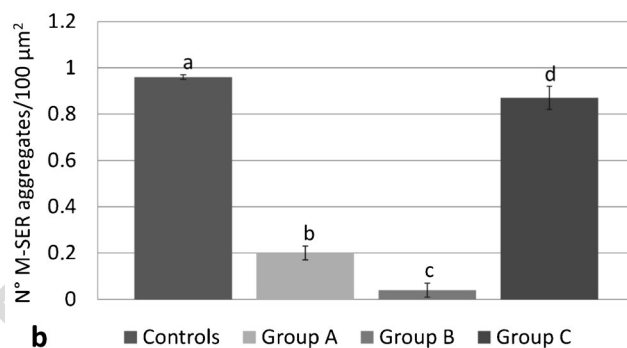
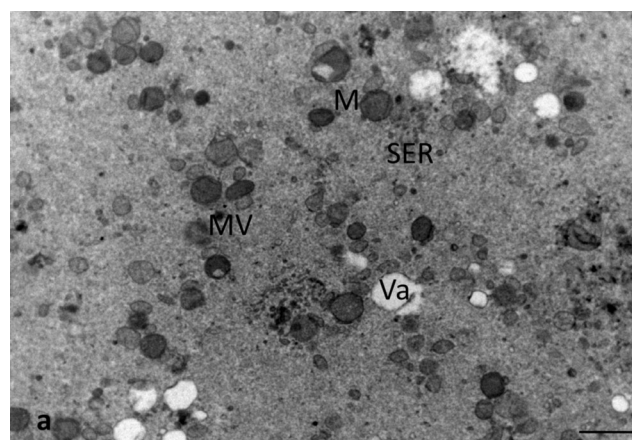


Fig. 4 Cryopreserved human metaphase II oocytes. Oocyte belonging to group A, a representative, panoramic picture of the ooplasm, as seen by transmission electron microscopy (Fig. 4a). Note the presence of typical mitochondria-smooth endoplasmic reticulum (*M-SER*) aggregates, together with numerous mitochondria (*M*) and mitochondria-vesicle (*MV*) complexes. *Va* vacuoles. Bar is: 1 μm (Fig. 4a). Fig. 4b: Number of *M-SER* aggregates (SER network diameter ≥ 0.5 μm) per 100 μm² of oocyte area. Values for each group are expressed as mean ± SD. Different letters indicate significant differences ($P < 0.05$)

395 Sometimes, secondary lysosomes were found in the proximity
 396 of the vacuoles (Fig. 3a). In the group B, the more pronounced
 397 vacuolization was often associated with an increased density
 398 of the cytoplasmic matrix (Fig. 3b).

399 A normal pattern of organelles was usually detected by
 400 TEM in ooplasm of the cryopreserved oocytes belonging
 401 to all experimental groups, including the ooplasmic areas
 402 adjacent to vacuoles (Figs. 3a,c; 4a). With this regard
 403 mitochondria, *M-SER* aggregates and *MV* complexes
 404 did not show overt qualitative ultrastructural changes if
 405 compared to those organelles and organelle associations
 406 found in control oocytes (Figs. 4a; 5a,b, inset). However,
 407 a percentage of small *M-SER* aggregates was found (with
 408 a diameter of SER networks of 1–2 μm), particularly in
 409 the oocytes belonging to groups A and B, whereas unusu-
 410 ally large *MV* complexes (up to 2.5 μm in vesicular di-
 411 ameter) were sometimes found in the oocytes belonging
 412 to group B.

TEM analysis also revealed that CGs were scanty, arranged
 in a discontinuous layer, and sometimes scarcely
 electron-dense in the cryopreserved oocytes belonging to all
 experimental groups in respect to those found in the control
 group (Fig. 6a–c). In addition, when a morphometric evalua-
 tion was performed, the mean number ± SD of CGs per 10 μm
 was 6.28 ± 1.12 (group A), 3.17 ± 0.28 (group B), 2.33 ± 0.50
 (group C), suggesting that CGs underwent an initial reduction
 at the beginning of rehydration (difference between control
 group and group A was statistically significant, $P < 0.001$)
 and further decreased in number as rehydration progressed
 (differences between groups A and B and between groups B
 and C were statistically significant, $P < 0.001$ and $P < 0.05$,
 respectively) (Fig. 6d).

Numerous microvilli were also seen bordering the
 oolemma and projecting into the PVS (Figs. 2d–f; 6a–c). In
 sections lying on appropriate planes, the PBI was detected in
 the PVS and the MII spindle was found in the ooplasm.

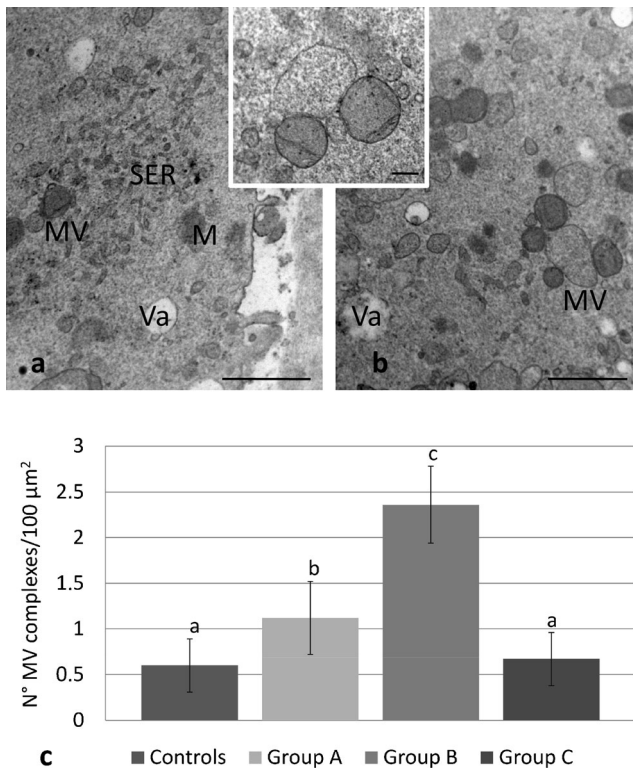


Fig. 5 Cryopreserved human metaphase II oocytes. Oocytes belonging to group A, representative pictures of mitochondria (M), mitochondria-smooth endoplasmic reticulum (M-SER) aggregates and mitochondria-vesicle (MV) complexes, as seen by transmission electron microscopy (Fig. 5a, b, inset). Note the presence of well preserved mitochondria and of typical MV complexes of various sizes. A high magnification of a MV complex is shown in the inset. Differently from vacuoles, the vesicles belonging to MV complexes are filled with a slightly electrondense material, are surrounded by an intact membrane and are closely associated to mitochondria. Va vacuoles. Bar is: 1 μm (Fig. 5a, b); 0.2 μm (inset). Fig. 5c: Number of MV complexes (vesicle diameter ≥ 0.5 μm) per 100 μm² of oocyte area. Values for each group are expressed as mean ± SD. Different letters indicate significant differences ($P < 0.05$)

431 **Discussion**

432 In humans, numerous studies suggest that post-thaw survival
 433 rates of oocytes that have undergone slow freezing are inferior
 434 to those of oocytes subjected to vitrification procedures [56].
 435 In addition, oocyte vitrification, compared to slow freezing,
 436 probably increases implantation and pregnancy rates [57, 58].
 437 The results, however, as reported in the Italian ART registry,
 438 are not homogeneous among clinics and protocols [59] since
 439 there is a wide variation in pregnancy rates among different
 440 centers [58]. Further, as it results from a general survey of the
 441 literature, the total number of women and pregnancies in the
 442 included trials were low and the evidence was limited by im-
 443 precision [57]. Moreover, ultrastructural dysmorphisms have
 444 been identified in both vitrified-warmed and frozen-thawed
 445 human MII oocytes, although at a different extent [17].

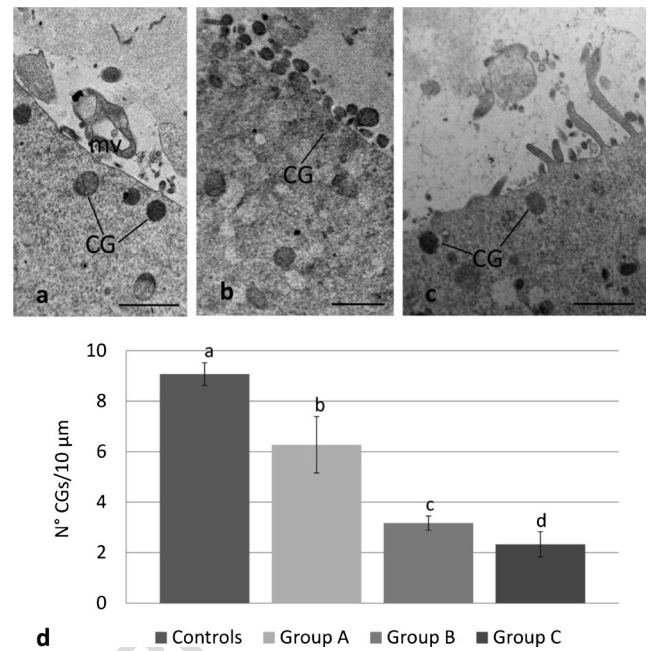


Fig. 6 Cryopreserved human metaphase II oocytes. In cryopreserved oocytes belonging to group A (Fig. 6a), B (Fig. 6b), and C (Fig. 6c), cortical granules (CG) appear by transmission electron microscopy sparse or isolated, forming a discontinuous layer. mv microvilli. Bar is: 1 μm (Fig. 6a–c). Fig. 6d: Number of CGs per 10 μm of oocyte linear surface profile. Values for each group are expressed as mean ± SD. Different letters indicate significant differences ($P < 0.05$)

In this regard, while vitrification seems to have a clear role
 in ART, continued research to establish optimal slow freezing
 methods for human MII oocytes seems required, which may
 assist in alleviating concerns over safety issues related to vit-
 rification, such as storage, transport and the use of very high
 cryoprotectant concentrations [60]. Slow freezing of oocytes
 can thus be a still valid tool in IVF practice when performed
 with a suitable protocol [61, 62].

The purpose of this study was firstly to investigate the
 phenomenon of vacuolization in human MII oocytes subject-
 ed to slow freezing, since presence and extent of this ultra-
 structural dysmorphism can be an important indicator of oocyte
 quality after cryopreservation. Secondly, we aimed to assess
 in the same oocytes the morphodynamics of typical oocyte
 organelles and organelle associations (M-SER aggregates,
 MV complexes, CGs) during freeze-thawing.

In particular, this is the first comprehensive study that de-
 scribes in detail, from both a qualitative and quantitative point
 of view, the structural and ultrastructural modifications occur-
 ring just after thawing, during the rehydration steps. In fact,
 although several factors have been successfully optimized in
 the protocols used to cryopreserve human oocytes, up to now,
 post-thaw rehydration conditions received a limited attention
 [5, 63, 64]. Different rehydration conditions seem also to in-
 fluence the survival of vitrified-warmed human oocytes [65].
 Rehydration could, indeed, sensitize the oocyte and make it

472 particularly vulnerable, since removal of the intracellular cryo-
473 protectant and the re-establishment of the original water con-
474 tent occurring during this procedure are both sources of os-
475 motic stress for the cell. In this view, it seems essential to
476 know in detail in which step/steps of the rehydration proce-
477 dure cryoinjuries may occur, in order to optimize rehydration
478 conditions, too.

479 **General features**

480 All the oocytes showed similar shape, dimensions, and overall
481 appearance, irrespective of their classification (control or ex-
482 perimental groups A, B, and C). Thus, neither freezing nor
483 thawing, including the different steps of post-thaw rehydra-
484 tion, seemed to associate with any significant variation in vol-
485 ume and/or general appearance of the oocytes. This feature
486 well correlates with previous observations on human mature
487 oocytes subjected to different protocols of slow freezing
488 [12–14, 17] or vitrification [15, 17, 55, 66], further empha-
489 sizing that current cryopreservation protocols do not significantly
490 impair oocyte general architecture.

491 By LM and TEM, the organelles appeared uniformly dis-
492 persed in the ooplasm of all the oocytes. However, organelle-
493 specific differences were found between control and frozen-
494 thawed oocytes as extent of vacuolization and differences in
495 the number of M-SER aggregates, MV complexes, and CGs.

496 **Vacuoles**

497 We found a slight to moderate vacuolization in the cryopre-
498 served oocytes belonging to all experimental groups. Vacuoles
499 were instead only occasionally present in the ooplasm of fresh
500 oocytes. In particular, vacuoles were already found in the
501 group A, after oocyte exposure to the thawing solution 1,
502 suggesting that they may form during freezing and/or at
503 thawing. Further, vacuoles increased in number as post-thaw
504 rehydration proceeded. They reached a maximum amount in
505 group B, after oocyte exposure to the thawing solution 2,
506 which contains the lowest concentration of PrOH during
507 PrOH step-wise dilution. Finally, vacuoles decreased again
508 in number at the end of the rehydration process (group C),
509 after oocyte exposure to the thawing solution 3, which is
510 PrOH-free. A measurable number of vacuoles, however, re-
511 main in the ooplasm of frozen-thawed oocytes, indicating that
512 their recovery is largely incomplete.

513 The abundance of vacuoles in frozen-thawed oocytes can
514 be interpreted as a manifestation of oocyte stress during cryo-
515 preservation. As introduced above, the degree of oocyte
516 vacuolization significantly increases by applying slow freez-
517 ing [12–14, 17, 67], whereas data on the presence of vacuoles
518 in vitrified oocytes appear still undefined and controversial
519 [15, 17, 66–68]. Taken together, however, all these data

indicate that vacuoles are less represented in vitrified than in 520
slow-frozen oocytes. 521

Vacuoles may derive from swelling and coalescence of 522
Golgi and/or SER membranes [21, 69], possibly associated 523
to cytoskeletal defects [14, 22]. In the mature oocyte SER 524
membranes, when transforming into vacuoles, become 525
interrupted and lose their close association with mitochondria, 526
typical for M-SER aggregates and MV complexes, acquiring 527
degenerative features [38]. Disruption of such a “molecular 528
hug” between mitochondria and SER [70] may contribute to 529
the occurrence of altered calcium transients in cryopreserved 530
oocyte. Peripheral vacuoles may also originate from 531
oolemmal invaginations [66] and/or clusters of endocytotic 532
vesicles forming in the oocyte cortex, as it occurs in oocytes 533
exposed to cryoprotectants only [12, 50]. In cryopreserved 534
oocytes vacuoles could also derive from altered, swollen mi- 535
tochondria [46, 47] or from the fusion of degenerating CGs, 536
associated to an extensive loss of the electron-dense granule 537
content [48]. 538

In this study, we sometimes identified secondary lyso- 539
somes adjacent to vacuoles. Vacuoles and lysosomes may 540
fuse, forming structures with a mixed content involved in 541
the degradation of ooplasmic material via autophagy [71]. 542
Some authors recently hypothesize that autophagic activation 543
in cryopreserved oocytes could be a natural, adaptative re- 544
sponse to “cold” stress [72, 73]. 545

In addition, we found that the more marked vacuolization 546
of the oocytes belonging to group B was often associated with 547
an increased density of the ooplasm. All these features are 548
similar to those found in post-mature, atretic oocytes unfertil- 549
ized after in vitro insemination [20]. This is a further prove 550
that regressive changes in cryopreserved oocytes are conse- 551
quent to altered cytoplasmic dynamics that are particularly 552
expressed when the cryoprotectant PrOH reaches its lowest 553
concentration in the second step of rehydration. 554

555 **M-SER aggregates and MV complexes**

In this study, we also found that significant variations, of op- 556
posite trend, occurred during freeze-thawing in size and num- 557
ber of M-SER aggregates and MV complexes. 558

In particular, M-SER aggregates, large and abundant in the 559
ooplasm of fresh controls, decreased in size and number after 560
thawing, particularly in the oocytes belonging to groups A and 561
B (first and intermediate stages of post-thaw rehydration), 562
indicating a special sensitivity of these aggregates to cryopro- 563
tectant exposure and, particularly, to PrOH withdrawal. On the 564
contrary, M-SER aggregates significantly increased in group 565
C, where PrOH was completely removed from the thawing 566
solution and a recovery of metabolic activities occurred. An 567
opposite trend was observed for MV complexes, and these 568
latter changes closely resemble those previously reported for 569
vacuoles. 570

571 On the basis of these findings, we suggest that ooplasmic
 572 membranes, whose dynamic structure may be regulated by
 573 cytoskeletal activity, as occurs in other cells [74], become
 574 capable of transforming into each other under an appropriate
 575 stimulus. According to this view, SER elements could dynam-
 576 ically acquire different shapes (tubules or vesicles) depending
 577 on the metabolic/structural needs of the cell, actually belong-
 578 ing to the same system of interconnected membranes. In fact,
 579 transitional figures with intermediate characteristics between
 580 tubules and vesicles have been observed by TEM [20]. In
 581 particular, we speculate that M-SER aggregates and small
 582 MV complexes, commonly found in the ooplasm of MII oo-
 583 cytes before freezing, can both give rise to numerous, large
 584 MV complexes after thawing and during rehydration, through
 585 a generous SER membrane reassembly. This is confirmed by
 586 previous studies in which the authors suggested that aging
 587 and/or prolonged culture can elicit a similar transition into
 588 the oocyte [17, 20, 38]. Large MV complexes are also present
 589 in GV oocytes that have reached MII stage after 24-h culture
 590 (in vitro matured oocytes) [75, 76]. Therefore, M-SER to MV
 591 transition does not seem related only to aging or culture period
 592 but can be also induced in cryopreserved oocytes by step-wise
 593 dilution of PrOH during post-thaw rehydration.

594 In this study, we also originally reported through a morpho-
 595 logical approach that a reversal of this phenomenon of mem-
 596 brane “recycling” occurs at the end of freeze-thawing, when
 597 the rehydration process is completed and culture conditions
 598 regain a more physiological state. As a consequence of this,
 599 the large vesicular component of MV complexes could shrink
 600 again to form small vesicles and tortuous, anastomosing SER
 601 tubules of M-SER aggregates. This well correlates with pre-
 602 vious reports on human oocytes subjected to slow freezing
 603 and treated with PrOH, which did not evidence at the end of
 604 the procedure of slow freezing any qualitative ultrastructural
 605 change of these aggregates in respect to fresh controls [12, 13,
 606 17]. However, from a quantitative morphometric analysis, we
 607 hereby reported a complete recovery only for MV complexes,
 608 whereas M-SER aggregates do not reach the number found in
 609 fresh controls, thus undergoing a reliable but partial recovery
 610 at the end of the rehydration process.

611 Cryopreservation has been reported to affect calcium oscil-
 612 lation in the human oocytes [77]. In this vein, since, as report-
 613 ed above, calcium levels in the oocyte are regulated by a
 614 correct cross-talk between mitochondria and associated
 615 ooplasmic membranes, membrane reassembling during rehy-
 616 dration may produce altered, although temporary, calcium
 617 transients, possibly interfering with oocyte competence to
 618 fertilization.

619 It seems also worth noting that, irrespective of the above
 620 described diffuse recycling of ooplasmic membranes, associ-
 621 ated mitochondria appear concerned neither by freezing nor
 622 by thawing and its sequential post-thaw rehydration steps,
 623 maintaining unaltered their ultrastructure. This finding further

reinforces the concept that both slow freezing and vitrification
 procedures do not significantly affect mitochondrial structure
 in human MII oocytes [12–15, 17].

627 Finally, on the basis of what discussed above, we cannot
 628 rule out that vacuoles and their membranes can play an active
 629 role in the membrane recycling that occurs during freeze-
 630 thawing. In fact, the membranes of M-SER aggregates and
 631 MV complexes could sometimes derail during their
 632 reassembling, becoming oriented toward vacuole
 633 transformation.

Cortical granules

634
 635 In this study, we revealed that CGs were scarce in the oocytes
 636 belonging to all experimental groups in respect to those found
 637 in the fresh control group. CGs gradually diminished as post-
 638 thaw rehydration progressed, reaching their lowest concentra-
 639 tion in group C and, thus, revealing the occurrence of a grad-
 640 ual but progressive loss during freeze-thawing. This feature
 641 well correlates with previous reports in which an ubiquitous
 642 reduction in number of CGs was found at the end of the cryo-
 643 preservation procedure, irrespective of the protocol applied
 644 (slow freezing, vitrification with closed or open devices)
 645 [12–15, 17]. A reduced amount and electron-density of CGs
 646 in cryopreserved oocytes may be due to the occurrence of a
 647 premature exocytosis of the CG content into the PVS with the
 648 consequent hardening of the inner aspect of the ZP, thus
 649 impairing oocyte fertilizability.

650 The novelty of our observations on CG morphodynamics
 651 during cryopreservation is related to the following consider-
 652 ations. Firstly, the whole freeze-thawing procedure may in-
 653 duce CG loss during cryopreservation. The reduction of CGs
 654 was in fact already evident in oocytes from group A. This
 655 means that the CG release could begin during freezing and/
 656 or at thawing. Secondly, the further reduction of CG observed
 657 in groups B and C indicates that the CG exocytosis does not
 658 stop after thawing, but continues throughout the following
 659 phases of rehydration. Such CG loss is thus the only phenom-
 660 enon, among those described in this study, apparently not
 661 subjected to any kind of recovery.

662 Several studies have shown that the mere exposure of ma-
 663 ture oocytes to cryoprotectants leads to a reduction in the
 664 number and electron-density of CGs [24, 50]. Therefore, also
 665 on the basis of these reports, we can further emphasize that
 666 the progressive CG loss reported in this study may be related
 667 not only to low temperatures but also to the processes of cryo-
 668 protectant addition (dehydration step) and removal (rehydration
 669 step). Cryoprotectant (PrOH) addition, in particular, has been
 670 reported to have a role in inducing a precocious oocyte acti-
 671 vation, and consequent CG exocytosis, by increasing calcium
 672 intake [25, 78]. More recently, Gualtieri et al. observed a sig-
 673 nificant delay of the recovery of intracellular calcium to basal
 674 levels in frozen-thawed oocytes [67]. According to the results

675 obtained in our work, it can be assumed that the concentration
676 of cytosolic calcium, once altered during dehydration, may
677 further increase during the rehydration and consequent
678 PrOH withdrawal, thus resulting in the described continuous,
679 progressive CG release.

680 In addition, the gradual loss of CGs during freeze-thawing
681 leads us to hypothesize that the membranes of the exocytosed
682 granules may not only be reintegrated in the oolemma but may
683 also, at least in part, contribute to the above described
684 ooplasmic membrane recycling.

685 **Conclusions and future perspectives**

686 In this report, we have originally reported that oocyte ultra-
687 structural dysmorphisms related to cryopreservation and possi-
688 bly responsible of low oocyte fertilizability not only occur
689 during freezing and thawing, in a strict sense, but also during
690 post-thaw rehydration. These cellular alterations, induced by
691 low temperatures and by osmotic and chemical forces pro-
692 duced during cycles of dehydration-rehydration as well, may
693 alter the distribution and activity of oocyte cellular
694 components.

695 In particular, although slow freezing appears to ensure a good
696 overall preservation of the oocyte; nevertheless, vacuolization
697 and CG release remain crucial limits. It seems also worth noting
698 that all systems of ooplasmic membranes appear significantly
699 affected by freeze-thawing but, except for CGs, their alterations
700 seem to undergo a partial or, more rarely, an almost complete
701 recovery after thawing, at the end of the rehydration process. In
702 addition, the observed variations in the number of M-SER ag-
703 gregates and MV complexes, occurring during freeze-thawing,
704 suggest that a dynamic process of transition between these two
705 forms of organelle associations may occur. At this regard, it
706 should not be excluded that vacuole and CG membranes, and
707 oolemma as well, may take part in the recycling mechanism.
708 Such shuttle of membranes, starting during freezing and/or at
709 thawing but mainly occurring during rehydration, may be relat-
710 ed to alterations of the cytoskeletal stiffness [79] presumably
711 due to PrOH administration and/or withdrawal [80, 81]. We
712 cannot exclude, of course, that the described membrane
713 restructuring is also related to calcium disturbances. From a
714 merely morphological point of view, this recycling reveals a sort
715 of morphogenetic multipotency of the oocyte cytomembranes,
716 possibly eliciting membrane turnover and delivery or clearance
717 of substances (CG content, cryoprotectants, calcium, other
718 solutes?), as postulated for other cells [82].

719 Finally, a similar ultrastructural approach could be
720 applied in the future to the study of the rehydration
721 process in slow-frozen oocytes undergoing rapid
722 warming [62] and in vitrified-warmed oocytes belonging
723 to both conventional and low-cryoprotectant vitrification
724 protocols [83].

Acknowledgments The present study was supported by grants from
the National Health Institute, Italian Ministry of Health and the Italian
Ministry of Education, University and Research (grants from *Sapienza*
University, Rome and University of L'Aquila, L'Aquila). The Authors
wish to acknowledge Mr. Ezio Battaglione of the Laboratory for
Electron Microscopy "Pietro M Motta," Department of Anatomy,
Histology, Forensic Medicine and Orthopaedics, *Sapienza* University,
Rome, for his contribution to sample preparation.

Compliance with ethical standards

Conflict of interest The authors declare that they have no conflict of
interest.

References

1. Cil AP, Seli E. Current trends and progress in clinical applica-
tions of oocyte cryopreservation. *Curr Opin Obstet Gynecol.*
2013;25:247–54.
2. Lockwood GM. Social egg freezing: the prospect of reproductive
'immortality' or a dangerous delusion? *Reprod Biomed Online.*
2011;23:334–40.
3. Hosseini SM, Nasr-Esfahani MH. What does the cryopreserved
oocyte look like? A fresh look at the characteristic oocyte fea-
tures following cryopreservation. *Reprod Biomed Online.*
2016;32:377–87.
4. Van Blerkom J, Davis PW. Cytogenetic, cellular, and developmen-
tal consequences of cryopreservation of immature and mature
mouse and human oocytes. *Microsc Res Tech.* 1994;27:165–93.
5. Cotichio G, Bonu MA, Sciajno R, Sereni E, Bianchi V, Borini A.
Truths and myths of oocyte sensitivity to controlled rate freezing.
Reprod Biomed Online. 2007;15:24–30.
6. Gardner DK, Sheehan CB, Rienzi L, Katz-Jaffe M, Larman MG.
Analysis of oocyte physiology to improve cryopreservation proce-
dures. *Theriogenology.* 2007;67:64–72.
7. Gook DA, Edgar DH. Human oocyte cryopreservation. *Hum*
Reprod Update. 2007;13:591–605.
8. Lornet J, Salle B. Ovarian and oocyte cryopreservation. *Curr Opin*
Obstet Gynecol. 2007;19:390–4.
9. Clark NA, Swain JE. Oocyte cryopreservation: searching for novel
improvement strategies. *J Assist Reprod Genet.* 2013;30:865–75.
10. Cotichio G, De Santis L, Rossi G, Borini A, Albertini D, Scaravelli
G, et al. Sucrose concentration influences the rate of human oocytes
with normal spindle and chromosome configurations after slow-
cooling cryopreservation. *Hum Reprod.* 2006;21:1771–6.
11. Cotichio G, Bromfield JJ, Sciajno R, Gambardella A, Scaravelli G,
Borini A, et al. Vitrification may increase the rate of chromosome
misalignment in the metaphase II spindle of human mature oocytes.
Reprod Biomed Online. 2009;19 Suppl 3:29–34.
12. Cotichio G, Borini A, Distratis V, Maione M, Scaravelli G,
Bianchi V, et al. Qualitative and morphometric analysis of the ul-
trastructure of human oocytes cryopreserved by two alternative
slow cooling protocols. *J Assist Reprod Genet.* 2010;27:131–40.
13. Nottola SA, Macchiarelli G, Cotichio G, Bianchi S, Cecconi S, De
Santis L, et al. Ultrastructure of human mature oocytes after slow
cooling cryopreservation using different sucrose concentrations.
Hum Reprod. 2007;22:1123–33.
14. Nottola SA, Cotichio G, De Santis L, Macchiarelli G, Maione M,
Bianchi S, et al. Ultrastructure of human mature oocytes after slow
cooling cryopreservation with ethylene glycol. *Reprod Biomed*
Online. 2008;17:368–77.

785 15. Nottola SA, Coticchio G, Sciajno R, Gambardella A, Maione M, 850
 786 Scaravelli G, et al. Ultrastructural markers of quality in human 851
 787 mature oocytes vitrified using cryoleaf and cryoloop. *Reprod* 852
 788 *Biomed Online*. 2009;19 Suppl 3:17–27.
 789 16. Bromfield JJ, Coticchio G, Hutt K, Sciajno R, Borini A, Albertini 853
 790 DF. Meiotic spindle dynamics in human oocytes following slow 854
 791 cooling cryopreservation. *Hum Reprod*. 2009;24:2114–23. 855
 792 17. Bianchi V, Macchiarelli G, Borini A, Lappi M, Cecconi S, Miglietta 856
 793 S, et al. Fine morphological assessment of quality of human mature 857
 794 oocytes after slow freezing or vitrification with a closed device: a 858
 795 comparative analysis. *Reprod Biol Endocrinol*. 2014;12:110. 859
 796 18. Camboni A, Martinez-Madrid B, Dolmans MM, Amorim CA, 860
 797 Nottola SA, Donnez J, et al. Preservation of fertility in young cancer 861
 798 patients: contribution of transmission electron microscopy. 862
 799 *Reprod Biomed Online*. 2008;17:136–50. 863
 800 19. Sundström P, Nilsson BO, Liedholm P, Larsson E. Ultrastructural 864
 801 characteristics of human oocytes fixed at follicular puncture or after 865
 802 culture. *J In Vitro Fert Embryo Transf*. 1985;2:195–206. 866
 803 20. Motta PM, Nottola SA, Micara G, Familiari G. Ultrastructure of 867
 804 human unfertilized oocytes and polyspermic embryos in an IVF-ET 868
 805 program. *Ann N Y Acad Sci*. 1988;541:367–83. 869
 806 21. Sathananthan AH, Ng S-C, Bongso A, Trounson A, Ratnam 870
 807 S. *Visual atlas of early human development for assisted repro-* 871
 808 *ductive technology*. Singapore: National University of 872
 809 Singapore; 1993. 873
 810 22. El Shafie M, Sousa M, Windt ML, Kruger TF. *An atlas of the* 874
 811 *ultrastructure of human oocytes*. New York: Parthenon 875
 812 Publishing; 2000. 876
 813 23. Makabe S, Van Blerkom J, Nottola SA, Naguro T. *Atlas of* 877
 814 *human female reproductive function. ovarian development to* 878
 815 *early embryogenesis after in vitro fertilization*. London: 879
 816 Taylor & Francis; 2006. 880
 817 24. Ghetler Y, Skutelsky E, Ben Nun I, Ben Dor L, Amihai D, Shalgi R. 881
 818 Human oocyte cryopreservation and the fate of cortical granules. 882
 819 *Fertil Steril*. 2006;86:210–6. 883
 820 25. Gualtieri R, Iaccarino M, Mollo V, Prisco M, Iaccarino S, Talevi R. 884
 821 Slow cooling of human oocytes: ultrastructural injuries and apoptotic 885
 822 status. *Fertil Steril*. 2009;91:1023–34. 886
 823 26. Sousa M, Cunha M, Silva J, Oliveira E, Pinho MJ, Almeida C, et al. 887
 824 Ultrastructural and cytogenetic analyses of mature human oocyte 888
 825 dysmorphisms with respect to clinical outcomes. *J Assist Reprod* 889
 826 *Genet*. 2016;33:1041–57. 890
 827 27. Fancsovits P, Murber A, Gilán ZT, Rigó Jr J, Urbancsek J. 891
 828 Human oocytes containing large cytoplasmic vacuoles can result in 892
 829 pregnancy and viable offspring. *Reprod Biomed Online*. 893
 830 2011;23:513–6. 894
 831 28. Setti AS, Figueira RC, Braga DP, Colturato SS, Iaconelli Jr A, 895
 832 Borges Jr E. Relationship between oocyte abnormal morphology and 896
 833 intracytoplasmic sperm injection outcomes: a meta-analysis. 897
 834 *Eur J Obstet Gynecol Reprod Biol*. 2011;159:364–70. 898
 835 29. Ebner T, Moser M, Sommergruber M, Gaiswinkler U, Shebl O, 899
 836 Jesacher K, et al. Occurrence and developmental consequences of 900
 837 vacuoles throughout preimplantation development. *Fertil Steril*. 901
 838 2005;83:1635–40. 902
 839 30. Wallbutton S, Kasraie J. Vacuolated oocytes: fertilization and embryonic 903
 840 arrest following intra-cytoplasmic sperm injection in a patient 904
 841 exhibiting persistent oocyte macro vacuolization—case report. 905
 842 *J Assist Reprod Genet*. 2010;27:183–8. 906
 843 31. Szöllösi D, Mandelbaum J, Plachot M, Salat-Baroux J, Cohen J. 907
 844 Ultrastructure of the human preovulatory oocyte. *J In Vitro Fert* 908
 845 *Embryo Transf*. 1986;3:232–42. 909
 846 32. Familiari G, Heyn R, Relucanti M, Nottola SA, Sathananthan AH. 910
 847 Ultrastructural dynamics of human reproduction, from ovulation to 911
 848 fertilization and early embryo development. *Int Rev Cytol*. 912
 849 2006;249:53–141. 913
 33. Motta PM, Nottola SA, Makabe S, Heyn R. Mitochondrial morphology 914
 2000;15 Suppl 2:129–47. 915
 34. Motta PM, Nottola SA, Familiari G, Makabe S, Stallone T, 916
 Macchiarelli G. Morphodynamics of the follicular-luteal complex 917
 during early ovarian development and reproductive life. *Int Rev* 918
Cytol. 2003;223:177–288. 919
 35. Dumollard R, Duchen M, Sartet C. Calcium signals and mitochondria 920
 at fertilisation. *Semin Cell Dev Biol*. 2006;17:314–23. 921
 36. Van Blerkom J. Mitochondrial function in the human oocyte and 922
 embryo and their role in developmental competence. 923
Mitochondrion. 2011;11:797–813. 924
 37. Nader N, Kulkarni RP, Dib M, Machaca K. How to make a good 925
 egg!: the need for remodeling of oocyte Ca(2+) signaling to mediate 926
 the egg-to-embryo transition. *Cell Calcium*. 2013;53:41–54. 927
 38. Bianchi S, Macchiarelli G, Micara G, Linari A, Boninsegna C, 928
 Aragona C, et al. Ultrastructural markers of quality are impaired 929
 in human metaphase II aged oocytes: a comparison between 930
 reproductive and in vitro aging. *J Assist Reprod Genet*. 931
 2015;32:1343–58. 932
 39. Otsuki J, Okada A, Morimoto K, Nagai Y, Kubo H. The relationship 933
 between pregnancy outcome and smooth endoplasmic reticulum 934
 clusters in MII human oocytes. *Hum Reprod*. 2004;19:1591–7. 935
 40. Sá R, Cunha M, Silva J, Luís A, Oliveira C, Teixeira Da Silva J, 936
 et al. Ultrastructure of tubular smooth endoplasmic reticulum 937
 aggregates in human metaphase II oocytes and clinical implications. 938
Fertil Steril. 2011;96:143–149.e7. 939
 41. Mateizel I, Van Landuyt L, Tournaye H, Verheyen G. Deliveries of 940
 normal healthy babies from embryos originating from oocytes 941
 showing the presence of smooth endoplasmic reticulum aggregates. 942
Hum Reprod. 2013;28:2111–7. 943
 42. Van Beirs N, Shaw-Jackson C, Rozenberg S, Autin C. Policy of ivf 944
 centres towards oocytes affected by smooth endoplasmic reticulum 945
 aggregates: a multicentre survey study. *J Assist Reprod Genet*. 946
 2015;32:945–50. 947
 43. Shaw-Jackson C, Thomas AL, Van Beirs N, Ameye L, Colin J, 948
 Bertrand E, et al. Oocytes affected by smooth endoplasmic reticulum 949
 aggregates: to discard or not to discard? *Arch Gynecol Obstet*. 950
 2016;294:175–84. 951
 44. Vincent C, Pickering SJ, Johnson MH. The hardening effect of 952
 dimethylsulphoxide on the mouse zona pellucida requires the presence 953
 of an oocyte and is associated with a reduction in the number 954
 of cortical granules present. *J Reprod Fertil*. 1990;89:253–9. 955
 45. Al Hasani S, Diedrich K. Oocyte storage. In: Grudzinskas JG, 956
 Yovich JL, editors. *Gametes—the oocyte*. Cambridge: Cambridge 957
 University Press; 1995. p. 376–94. 958
 46. Fuku E, Xia L, Downey BR. Ultrastructural changes in bovine 959
 oocytes cryopreserved by vitrification. *Cryobiology*. 960
 1995;32:139–56. 961
 47. Fuku EJ, Liu J, Downey BR. In vitro viability and ultrastructural 962
 changes in bovine oocytes treated with a vitrification solution. *Mol* 963
Reprod Dev. 1995;40:177–85. 964
 48. Hyttel P, Vajta G, Callesen H. Vitrification of bovine oocytes with 965
 the open pulled straw method: ultrastructural consequences. *Mol* 966
Reprod Dev. 2000;56:80–8. 967
 49. Valojerdi MR, Salehnia M. Developmental potential and ultrastructural 968
 injuries of metaphase II (MII) mouse oocytes after slow freezing 969
 or vitrification. *J Assist Reprod Genet*. 2005;22:119–27. 970
 50. Schalkoff ME, Oskowitz SP, Powers RD. Ultrastructural observations 971
 of human and mouse oocytes treated with cryopreservatives. 972
Biol Reprod. 1989;40:379–93. 973
 51. Jones A, Van Blerkom J, Davis P, Toledo AA. Cryopreservation of 974
 metaphase II human oocytes effects mitochondrial membrane potential: 975
 implications for developmental competence. *Hum Reprod*. 976
 2004;19:1861–6. 977


915 52. Borini A, Levi Setti PE, Anserini P, De Luca R, De Santis L, Porcu
916 E, et al. Multicenter observational study on slow-cooling oocyte
917 cryopreservation: clinical outcome. *Fertil Steril*. 2010;94:1662–8.
918 53. Ebner T, Moser M, Sommergruber M, Tews G. Selection based on
919 morphological assessment of oocytes and embryos at different
920 stages of preimplantation development: a review. *Hum Reprod*
921 *Update*. 2003;9:251–62.
922 54. Nottola SA, Heyn R, Camboni A, Correr S, Macchiarelli G.
923 Ultrastructural characteristics of human granulosa cells in a
924 coculture system for in vitro fertilization. *Microsc Res Tech*.
925 2006;69:508–16.
926 55. Khalili MA, Maione M, Palmerini MG, Bianchi S, Macchiarelli G,
927 Nottola SA. Ultrastructure of human mature oocytes after vitrification.
928 *Eur J Histochem*. 2012;56:e38. doi:10.4081/ejh.2012.e38.
929 56. Practice Committees of American Society for Reproductive
930 Medicine; Society for Assisted Reproductive Technology. Mature
931 oocyte cryopreservation: a guideline. *Fertil Steril*. 2013;99:37–43.
932 57. Glujovsky D, Riestra B, Sueldo C, Fiszbajn G, Repping S,
933 Nodar F, et al. Vitrification versus slow freezing for women
934 undergoing oocyte cryopreservation. *Cochrane Database Syst*
935 *Rev*. 2014;9:CD010047.
936 58. Levi-Setti PE, Borini A, Patrizio P, Bolli S, Vigiliano V, De Luca R,
937 et al. ART results with frozen oocytes: data from the Italian ART
938 registry (2005–2013). *J Assist Reprod Genet*. 2016;33:123–8.
939 59. Levi Setti PE, Porcu E, Patrizio P, Vigiliano V, de Luca R, d’Aloja P,
940 et al. Human oocyte cryopreservation with slow freezing versus
941 vitrification. Results from the national Italian registry data, 2007–
942 2011. *Fertil Steril*. 2014;102:90–95.e2.
943 60. Edgar DH, Gook DA. A critical appraisal of cryopreservation (slow
944 cooling versus vitrification) of human oocytes and embryos. *Hum*
945 *Reprod Update*. 2012;18:536–54.
946 61. Bianchi V, Lappi M, Bonu MA, Borini A. Oocyte slow freezing
947 using a 0.2–0.3 M sucrose concentration protocol: is it really the
948 time to trash the cryopreservation machine? *Fertil Steril*.
949 2012;97:1101–7.
950 62. Parmegiani L, Tatone C, Cognigni GE, Bernardi S, Troilo E,
951 Arnone A, et al. Rapid warming increases survival of slow-
952 frozen sibling oocytes: a step towards a single warming procedure
953 irrespective of the freezing protocol? *Reprod Biomed*
954 *Online*. 2014;28:614–23.
955 63. Stachecki JJ, Willadsen SM. Cryopreservation of mouse oocytes
956 using a medium with low sodium content: effect of plunge temper-
957 ature. *Cryobiology*. 2000;40:4–12.
958 64. Tao T, Del Valle A. Human oocyte and ovarian tissue cryopreser-
959 vation and its application. *J Assist Reprod Genet*. 2008;25:287–96.
960 65. Shanshan G, Mei L, Keliang W, Yan S, Rong T, Zi-Jiang C.
961 Effect of different rehydration temperatures on the survival of
962 human vitrified-warmed oocytes. *J Assist Reprod Genet*.
963 2015;32:1197–203.
964 66. Palmerini MG, Antinori M, Maione M, Cerusico F, Versaci C,
965 Nottola SA, et al. Ultrastructure of immature and mature human
966 oocytes after cryotop vitrification. *J Reprod Dev*. 2014;60:411–20.
1019
67. Gualtieri R, Mollo V, Barbato V, Fiorentino I, Iaccarino M, Talevi
967 R. Ultrastructure and intracellular calcium response during activa-
968 tion in vitrified and slow-frozen human oocytes. *Hum Reprod*.
969 2011;26:2452–60.
970 68. Bonetti A, Cervi M, Tomei F, Marchini M, Ortolani F, Manno
971 M. Ultrastructural evaluation of human metaphase II oocytes
972 after vitrification: closed versus open devices. *Fertil Steril*.
973 2011;95:928–35.
974 69. Sathananthan AH, Trounson A, Freeman L. Morphology and
975 fertilizability of frozen human oocytes. *Gamete Res*.
976 1987;16:343–54.
977 70. Kormann B. The molecular hug between the ER and the mito-
978 chondria. *Curr Opin Cell Biol*. 2013;25:443–8.
979 71. Kroemer G, Galluzzi L, Vandenabeele P, Abrams J, Alnemri ES,
980 Baehrecke EH, et al. Classification of cell death: recommendations
981 of the Nomenclature Committee on Cell Death 2009. *Cell Death*
982 *Differ*. 2009;16:3–11.
983 72. Bang S, Shin H, Song H, Suh CS, Lim HJ. Autophagic activation in
984 vitrified-warmed mouse oocytes. *Reproduction*. 2014;148:11–9.
985 73. Bang S, Lee GK, Shin H, Suh CS, Lim HJ. Vitrification, in vitro
986 fertilization, and development of Atg7 deficient mouse oocytes.
987 *Clin Exp Reprod Med*. 2016;43:9–14.
988 74. Cheng JP, Lane JD. Organelle dynamics and membrane trafficking
989 in apoptosis and autophagy. *Histol Histopathol*. 2010;25:1457–72.
990 75. Shahedi A, Hosseini A, Khalili MA, Norouzzian M, Salehi M,
991 Piriaei A, et al. The effect of vitrification on ultrastructure of human
992 in vitro matured germinal vesicle oocytes. *Eur J Obstet Gynecol*
993 *Reprod Biol*. 2013;167:69–75.
994 76. Coticchio G, Dal Canto M, Fadini R, Mignini Renzini M,
995 Guglielmo MC, Miglietta S, et al. Ultrastructure of human oocytes
996 after in vitro maturation. *Mol Hum Reprod*. 2016;22:110–8.
997 77. Nikiforaki D, Vanden Meerschaut F, Qian C, De Croo I, Lu Y,
998 Deroo T, et al. Oocyte cryopreservation and in vitro culture affect
999 calcium signalling during human fertilization. *Hum Reprod*.
1000 2014;29:29–40.
1001 78. Larman MG, Katz-Jaffe MG, Sheehan CB, Gardner DK. 1,2-
1002 propanediol and the type of cryopreservation procedure adversely
1003 affect mouse oocyte physiology. *Hum Reprod*. 2007;22:250–9.
1004 79. Ragoonanan V, Less R, Aksan A. Response of the cell membrane-
1005 cytoskeleton complex to osmotic and freeze/thaw stresses. Part 2:
1006 The link between the state of the membrane-cytoskeleton complex
1007 and the cellular damage. *Cryobiology*. 2013;66:96–104.
1008 80. Vincent C, Garnier V, Heyman Y, Renard JP. Solvent effects on
1009 cytoskeletal organization and in-vivo survival after freezing of rab-
1010 bit oocytes. *J Reprod Fertil*. 1989;87:809–20.
1011 81. Joly C, Bchini O, Boulekbache H, Testart J, Maro B. Effects of 1,2-
1012 propanediol on the cytoskeletal organization of the mouse oocyte.
1013 *Hum Reprod*. 1992;7:374–8.
1014 82. Steinman RM, Mellman IS, Muller WA, Cohn ZA. Endocytosis
1015 and the recycling of plasma membrane. *J Cell Biol*. 1983;96:1–27.
1016 83. Choi JK, Huang H, He X. Improved low-CPA vitrification of mouse
1017 oocytes using quartz microcapillary. *Cryobiology*. 2015;70:269–72.
1018

AUTHOR QUERIES

AUTHOR PLEASE ANSWER ALL QUERIES.

Q1. Please check if the affiliations are presented correctly. 

Q2. Capsule is mandatory. Please provide.

Q3. Please check if the references are presented correctly. 



UNCORRECTED PROOF